International Journal of Chemical Sciences

Research | Vol 17 Iss 1
DOI: 10.21767/0972-768X.1000306

Adsorption of Cd^{2+} ions from Synthetic Water by Magnetic Core Shell Nanocomposite $SiO_2/FeO/Fe_3O_4/SiO_2$

Elfiky AA[1*], Fathy M[1], Eltorgoman AM[2] and Moghny TA[1]

[1]Department of Applications, Egyptian Petroleum Research Institute (EPRI), Ahmed El-Zomer, Nasr City, Box. No, Cairo, Egypt

[2]Faculty of Science, Menofeya University, Gamal Abd El-Nasr St. Shebin El Koum-Menofeya, Egypt

[*]**Corresponding author:** Elfiky AA, Department of Applications, Egyptian Petroleum Research Institute (EPRI), Ahmed El-Zomer, Nasr City, P.O. Box. No, Cairo, Egypt, Tel: +202-22747847; E-mail: aya.elfiky91@yahoo.com

Received: March 06, 2019; **Accepted:** March 30, 2019; **Published:** April 05, 2019

Abstract

The magnetic silica core shell nanocomposite $SiO_2/FeO/Fe_3O_4/SiO_2$, which designated by (AS/Fe/AS), was synthesized and characterized by chemical analyses, FTIR, XRD, SEM, HR-TEM. The magnetic properties of (AS/Fe/AS) as a function of magnetic field, temperature, and time was measured using Vibrating Sample Magnetometer (VSM). Finally, the chemical purity and their stoichiometry of magnetic core shell SiO_2 /FeO/ Fe_3O_4/ SiO_2 (AS/Fe/AS) were done by Energy-dispersive X-ray spectroscopy (EDX). Also, the kinetic and isotherm studied were carried out by considering some important factors such as temperature, time and initial metal concentration on the adsorption capacity of (AS/Fe/AS) to remove Cd^{2+} ions from synthetic polluted water. The result confirms that we have successfully synthesized a new high-purity magnetite nanocomposite (AS/Fe/AS), which characterized by the presence of highly saturated magnetization and intensively black color. Also, we found that the kinetic and isotherm studied revealed that the adsorption kinetics and equilibrium data were best fitted by pseudo-second order kinetic model and Freundlich adsorption isotherm.

Keywords: Organic pollutants; Nanocomposite; Spectroscopy; Nanoparticles; Metal contamination

Introduction

Increasing the discharge of industrial waste water containing a large amount of heavy metals such as copper (II), Cd (II) and Pb (II) and organic pollutants in water or soil, is one of the biggest problems facing our societies at present, which in turn threat the environment and public health, because of their severe toxicity, if not discharged without proper treatment [1]. Cadmium is one of the most toxic elements that cause serious mutilation to the reproductive system, kidneys, liver, nervous system and the brain [2]. The maximum daily detection of cadmium from all sources (water, food and air) ranges from 1.0 to 1.2 μg/kg of body mass. In addition, the permissible limit of cadmium in drinking water must be not exceeded than 0.005 (mg/L). Thereby, the periodical examination must be applying on the water treatment equipment to ensure that the

Citation: Elfiky AA, Fathy M, Eltorgoman AM, et al. Adsorption of Cd^{2+} ions from synthetic water by Magnetic Core Shell Nanocomposite $SiO_2/FeO/ Fe_3O_4/ SiO_2$. Int J Chem Sci. 2019;17(1):306

permissible limit of feed water conditions and equipment capacity are not exceeded [3]. Many methods had been used to remove heavy metals, such as chemical precipitation [4], electro-flotation, ion-exchange and reverse osmosis; unfortunately, all of these methods are uneconomic in many developing countries. Meanwhile, the adsorption method is characterized by being more efficient, relatively economical, flexibility of design, ease of operation and the secondary waste such as sludge did not form. A wide range of adsorbents such as activated carbons, metal oxide composite, miso pours silica nanoparticle, polymer composite, and mixed organic inorganic nanocomposite have been developed and tested as adsorbents to remove Cd^{2+} ions and others from wastewaters [5,6]. The magnetic nanoparticles such as Fe_2 and its oxide (Fe_3O_4), showed a high metal adsorption capacity, high dispersion degree and super para magnetism behavior compared to their bulk form [7]. Therefore, and due to their properties, they can be applied on a wide field such as electronics, biotechnology, medicine, heavy oil upgrading, air pollution, and for water treatment [8].

Magnetic core shell silica nanocomposite is currently interest due to their potential applications in water treatment and remediation, hetero- and photo catalysis, optics and ultra-high-density magnetic storage. In addition, the silica Nanocomposite that having distinct core and shell magnetic phases [9], are very actively being investigated for magnetic sorbents and other potential applications such as removal of heavy metals from polluted water [6]. Silica-based magnetic nanoparticles have been various advantages choosing over for encapsulating magnetic nano-particles. Various silica particles with different mesh size have been used for the immobilization of important enzyme and bio-catalysis in organic media. Silica immobilized enzymes have been used for the synthesis of flavor esters and various medically important esters in organic solvents. It exposes silanol surface groups which can be derivative with a number of functional groups. It has optical transparency. It can prevent luminescence quenching by providing barrier in between the fluorophore and magnetic core. Due to their degradation stability, biocompatibility and hydrophilic character makes its application in environment and biomedical. They can be made by spray-drying, aerosol pyrolysis, sol–gel processes, and micro emulsion polymerization. A graphic representation of silica-based magnetic nano-particles has been depicted in FIG. 1. Different magnetic nano-composites made with their applications in previous studies are given in the reference [10,11].

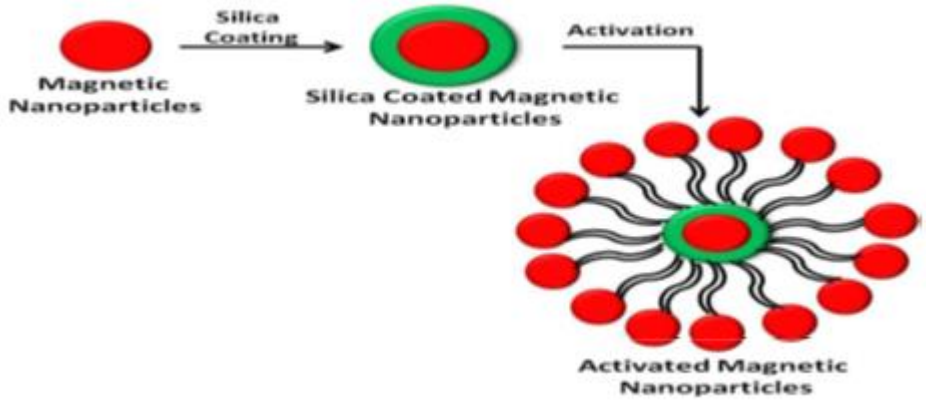

FIG. 1. **Mechanism of silica-based magnetic nano-particles.**

We aim to synthesize of magnetic core shell nanocomposite SiO_2/FeO/Fe_3O_4/ SiO_2 (AS/Fe/AS), via mixing of iron oxide with silica, to adsorb Cd^{2+} ions from synthetic polluted water, then characterize the prepared (AS/Fe/AS) by FTIR spectroscopy, XRD, TGA, chemical analyses, and by SEM, HR-TEM electron microscopy. Also, we aim to study the adsorption capacity of

Cd^{2+} ions onto AS/Fe/AS at different contact time, pH, adsorbent dose and initial Cd^{2+} ions concentration. Finally, we determine the appropriate adsorption isotherm and kinetics parameters of Cd^{2+} ions onto (AS/Fe/AS).

Experimental Procedure

Materials

Ethanol, cadmium nitrate tetrahydrate and ferric chloride, amorphous silica gel (0.06-0.2 mm, 60A) were all obtained from Sigma-Aldrich. TEOS (Tetraethyl ortho-silicate or tetra-ethoxysilane) is a colorless liquid degrades in water, with chemical formula of Si $(OC_2H_5)_4$, was obtained from Sigma-Aldrich. The other chemicals that used were analytical grade. The stock cadmium solution was diluted at appropriate proportions, to prepare different initial cadmium concentrations. All glassware was kept overnight in a 10% (v/v) HNO_3 solution to prevent laboratory glassware from metal contamination. Stock solutions were prepared daily by dissolving in distilled water.

Preparation of magnetic silica core shell nanocomposite FeO/ Fe_3O_4/ SiO_2 (Fe/AS)

The suspended silica was prepared by distributing 20 g of amorphous silica gel (AS) (0.06-0.2 mm, 60A) in 250 ml distilled water with stirring at 250-300 rpm. The iron chloride solution was prepared by solubilizing of 10 grams of $FeCl_3$ in 50 ml distilled water. Then iron chloride solution was added drop wise with stirring for 20 minutes to the suspended silica, for obtaining the adsorbed magnetic silica composite [12] and was precipitate by adding sodium hydroxide solution then left the suspended solution for 2 hours. 100 ml of 0.3 M $NaBH_4$ was added drop wise to magnetic silica composite with vigorous stirring at 4000 rpm for 40 min, to reduce the trivalent iron oxide producing surface cover zero valent iron (Fe/AS). Then filtrate the precipitate and washed it with 250 to 500 ml distilled water until it becomes neutral, then dried in the oven at 150ºC for 2 hours to obtain calcinated Fe/AS nanocomposite as shown in FIG. 2 [13].

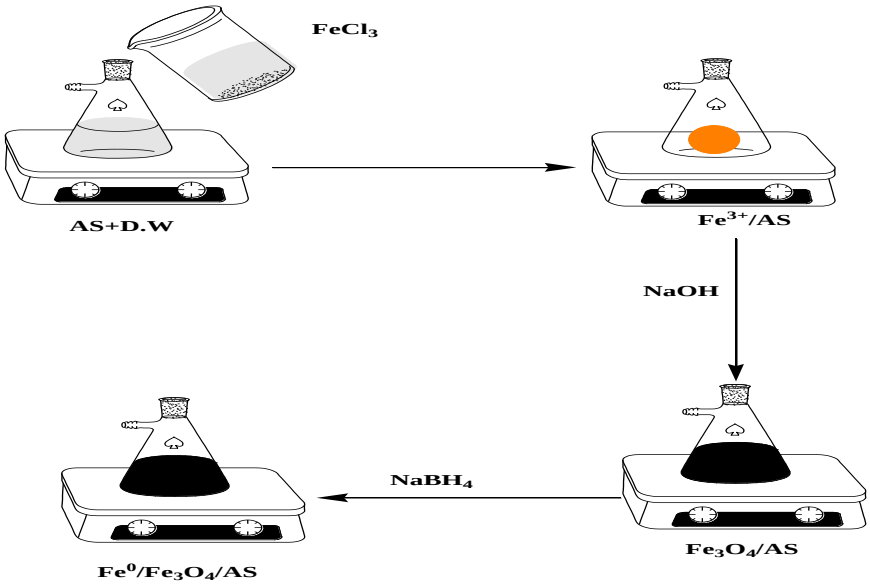

FIG. 2. **Preparation of magnetic silica nanocomposite FeO/Fe_3O_4/SiO_2 (Fe/AS).**

Preparation of magnetic core shell SiO_2/FeO/ Fe_3O_4/ SiO_2 nanocomposite (AS/Fe/AS)

2 g of the prepared Fe/AS nanocomposite was added to 50 ml of TEOS solubilized in 150 ml ethanol and then precipitate by 0.5% w/v sodium hydroxide solution with stirring at 60°C for one hour and left. The precipitate was washed with distilled water until it becomes neutral and leaves to dry at 80°C to obtain on a dark brown gel, then leave for 1 hour with stirring at room temperature and dried in a muffle furnace. After that, the dark brown gel was calcinated at 200°C for 8 hours for oxidation all the hydroxide Fe $(OH)_3$ and partial oxides to iron oxide Fe_3O_4 in presence of FeO spots within the latex of magnetite, finally, a black magnetite core shell SiO_2/FeO/Fe_3O_4/SiO_2 nono-composite (AS/Fe/AS) was obtained as shown in FIG. 3 [14].

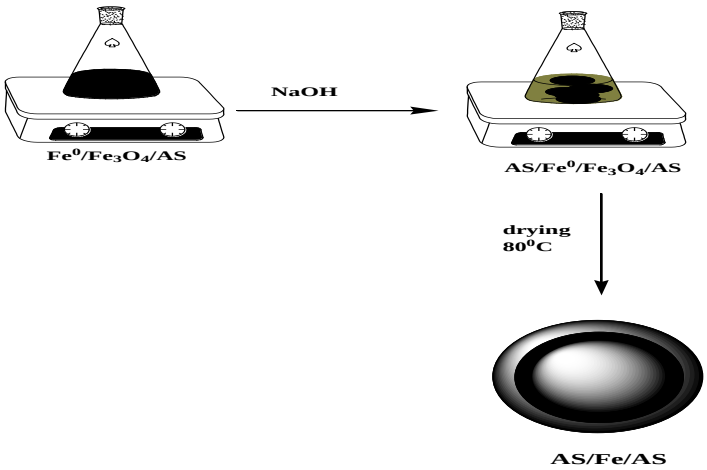

FIG. 3. **Preparation of magnetic core shell SiO_2 /FeO/ Fe_3O_4/ SiO_2 (AS/Fe/AS).**

Methods of characterization

Chemical structure of the AS/Fe/AS nanocomposite were confirmed by using FTIR (Nicolet IS-10 FT-IR), where X-ray diffraction (XRD) (Shimadzu XRD Model 6000) was used to describe its structure phases and average size. Additionally, the surface morphology (SEM and HR-TEM) were characterized using SEM, Jeol, Model JSM5300 at 15 Kev. The magnetic properties of (AS/Fe/AS) as a function of magnetic field, temperature, and time was measured using BHV-55. Vibrating Sample Magnetometer (VSM). Finally, the elemental analysis or chemical characterization or chemical purity and their stoichiometry of magnetic core shell SiO_2/FeO/Fe_3O_4/SiO_2 (AS/Fe/AS) were done by Energy-dispersive X-ray spectroscopy (EDX) (EDX, Kevex, Delta Class I).

Adsorption procedure

Adsorption tests were performed in batch-mode according to the procedures described by Fathy and Elsayed [15], and the resulted data were analyzed using both of pseudo-first-order and pseudo-second-order kinetic models as tabulate in TABLE 1. The adsorption capacity and the removal percentage (R%) of Cd^{2+} ions onto (AS/Fe/AS) were measured at wavelength of 554 nm.

Adsorption isotherms

Adsorption isotherms of AS/Fe/AS nanocomposite were conducted by varying the initial Cd^{2+} ions concentration from 10 to 300 mg/L at different temperatures (298-345 K) and pH 6.5. The resulted data were analyzed by applying Langmuir and Freundlich isotherm models and were given in TABLE 2.

Results and Discussion

FTIR analysis

The FTIR spectrum of magnetic silica core shell nanocomposite $SiO_2/FeO/Fe_3O_4/SiO_2$which designated by (AS/Fe/AS) is given in FIG. 4 and shows the presence of absorption bands at 3650-3200 cm^{-1} correspond to O–H stretching vibration mode of Fe–OH bond, with the presence of two bands at approximately 1070, and 600 cm^{-1}, which are assigned to the stretching and bending vibration modes of Si–O–Si surface, respectively, whereas, the band observed at 460 cm^{-1} is assigned to Fe–O stretching bond. The existence of SiO_2 layers in the spectrum of can be realized by the Si–O–Si stretching vibration at 1070 cm^{-1}, as well as the Fe–O–Si stretching vibration at 1250-1050 cm^{-1}. The result confirms the successfully synthesized of new high-purity magnetite nanocomposite (AS/Fe/AS), characterized with the presence of highly saturated magnetization and intensively black color.

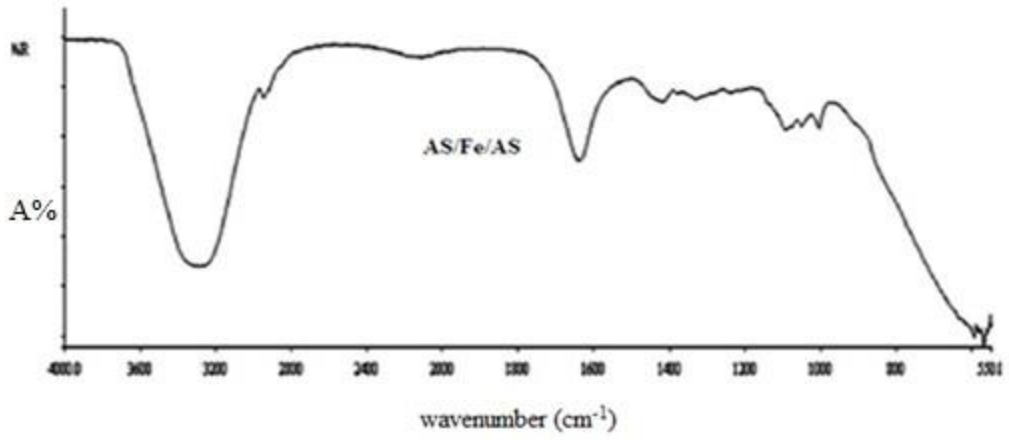

FIG. 4. **FTIR spectrum of AS/Fe/AS nanocomposite.**

Characterization using XRD

Three X-ray diffraction spectrum patterns are shown in FIG. 5 and named by (AS), FeO and (AS/Fe/AS), respectively. The interpretation of these spectra is as follows:

The XRD peak of AS indicated the presence of only amorphous peak characterized with the equivalent Bragg angle at 2θ=21.8º, we may note there are tetragonal a-crystobalite and a small fraction of monoclinic tridymite were obtained [16]. Secondary, the XRD pattern of magnetic Fe_3O_4 which named by FeO has the spinal structure with characteristic peaks at 2θ=27.47, 31.85°, 45.61° and 56.61° correspond to Fe_3O_4 crystal plane of (2 2 0), (3 1 1), (4 0 0), (4 2 2), and (5 1 1), respectively (JCPDS Card No. 019-0629), and their nano-crystalline size found around 40 nm as calculate by Scherrer equation.

Finally, the XRD pattern of the prepared magnetic core shell nanocomposite (AS/Fe/AS), exhibit the presence of both Fe_3O_4 crystal phase and SiO_2 amorphous phase [17]. Also, the Fe_3O_4 crystal structure changed and shifted to lower degree with respect to magnetic nanoparticles after coating with SiO_2 mesoporous shell (JCPDS no. 33-1161). This result can be explained by the unequal distribution of magnetic particles on AS/Fe/AS surface, beside the presence of silica sheet on the surface of the magnetic particles, beside the presence of silica particles on the core [18].

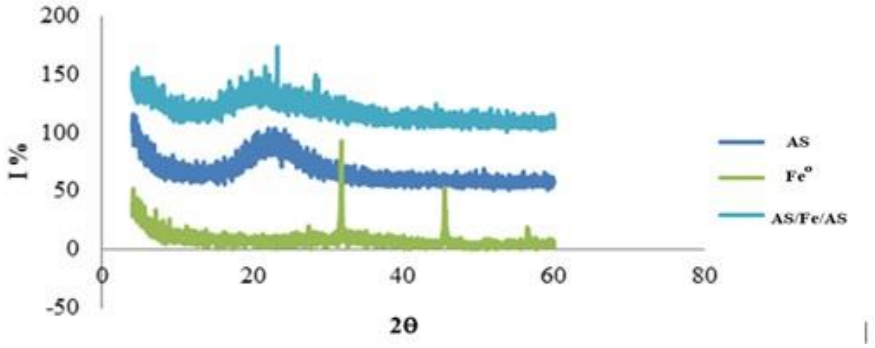

FIG. 5. **The XRD spectrum of amorphous silica particles (AS), Fe°, and the prepared magnetic core shell nanocomposite (AS/Fe/AS).**

Scanning electron microscopy of magnetic nanocomposite (AS/Fe/AS)

SEM image of **(**AS/Fe/AS) in FIG. 6 indicates that the first homogeneous cover layer of FeO and Fe_3O_4 were formed on the silica spheres. Also, we can see in the top left image in FIG. 6, the second thin silicon dioxide layer was formed on magnetic iron silica composite. However, the formation of thin silica shells on the nano-FeO/Fe_3O_4 particles returned rough surface and the resultant products showed nearly wide dispersed spheres 700-1500 µm-sized silica core.

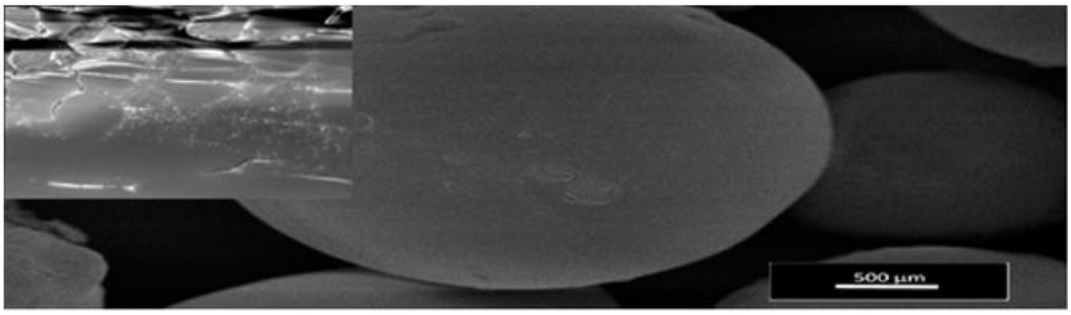

FIG. 6. **SEM images of magnetic nanocomposite AS/Fe/AS.**

The magnetic properties of the prepared magnetic nanocomposite AS/Fe/AS

The magnetic properties of the prepared FeO and magnetic nanocomposite (AS/Fe/AS) curves were measured using Vibrating Sample Magnetometer (VSM) and presented in FIG. 7. Clearly, the field-dependent magnetization curves of FeO and (AS/Fe/AS) measured at 300 K, exhibited a typical super- paramagnetic and no hysteresis was observed in low fields, otherwise, the magnetic saturation value of FeO and AS/Fe/AS are 9 emu/g and 48 emu/g, respectively, i.e., the sharply decreases of magnetic saturation value of FeO, can be attributed to increase of magnetic oxides and FeO mass. Additionally, as shown in FIG. 6, SiO_2/FeO/ Fe_3O_4/ SiO_2 with super paramagnetic characteristic and high magnetization value could quickly respond to external magnetic field and re-disperse in aqueous solution once the external magnetic field was removed and with gentle shaking or sonication.

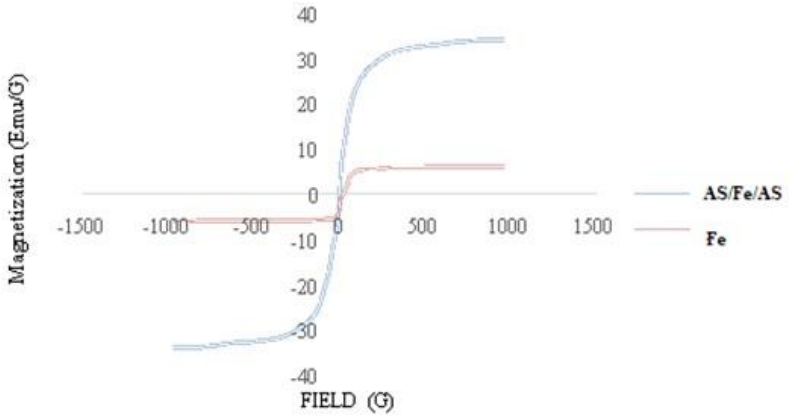

FIG. 7. **VSM of the prepared FeO and magnetic nano-composite AS/Fe/AS at 300 K.**

HR-TEM of magnetic nanocomposite (AS/Fe/AS)

Its observed from the HR-TEM of (AS/Fe/AS) in FIG. 8, that the size of silica nanocomposite coated with shell synthesized from TEOS ranged between 500-600 nm, and our results are very good compatible with the reference [16]. On the other hand, it is clear from the upper lift side on magnified FIG. 7, that the nano-FeO/Fe_3O_4 core are randomly distributed and their size ranges between 150-200 nm. Also, a thin silica shell was appeared as a smooth surface without any Flexural or aliasing on the surface of nano-FeO/Fe_3O_4 core, this indicated on the formation of thin layer from SiO_2 core–shell with uniform spherical morphology.

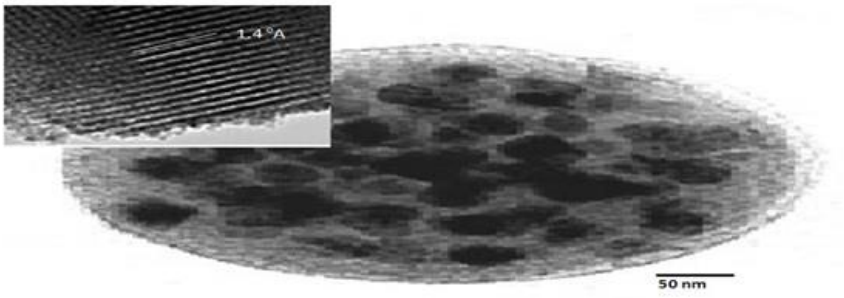

FIG. 8. **Particle morphology and surface feature of core shell AS/Fe/AS magnetic nanocomposite.**

EDX spectra of magnetic nanocomposite (AS/Fe/AS)

The EDX spectrum given in FIG. 9a shows the presence of Fe and O as the only elementary components of Fe_3O_4 nanoparticles. EDX spectrum of Fe_3O_4/SiO_2 (FIG. 9b) shows the elemental compositions are (Fe, O and Si) of core-shell nanoparticles. The EDX spectrum of SiO_2/FeO/ Fe_3O_4/ SiO_2 (FIG. 9c) shows the elemental compositions are (Fe, Si, O and FeO) of magnetic nanocomposite.

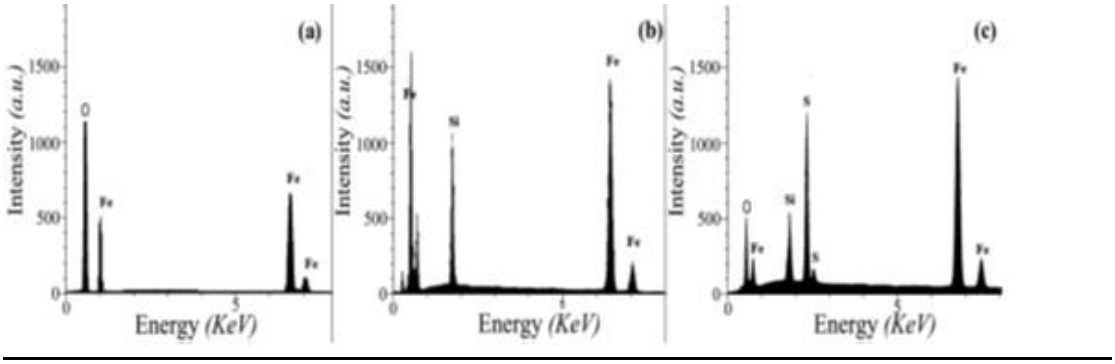

FIG. 9. **EDX spectra of (a) Fe_3O_4, (b) Fe_3O_4/SiO_2 and ($cSiO_2/FeO/ Fe_3O_4/ SiO_2$.**

Evaluation of adsorption performance

Effect of adsorbent dose: As shown in FIG. 10, the minimum Cd^{2+} ions removal, was 53.12% at 0.05 g of nanocomposite, whereas, the maximum Cd^{2+} ions removal value was 85.52% at 0.25 g of AS/Fe/AS nanocomposite. The increase in adsorption with increasing the amount of meso-porous silica composite dose may be attributed to the fact of the availability of more adsorption sites, i.e., increasing the available surface area to complete the adsorption process [19].

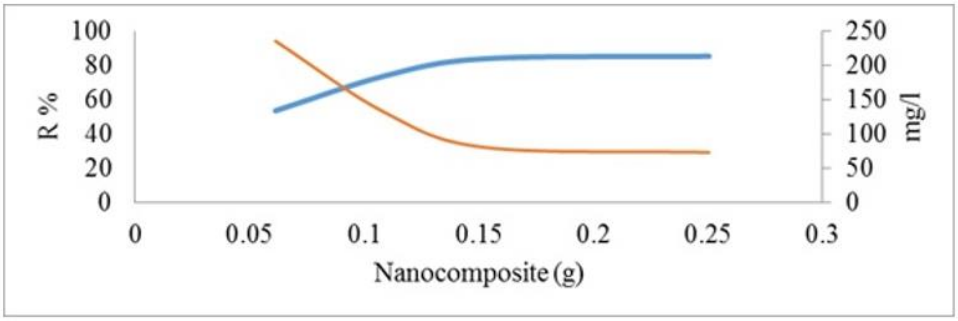

FIG. 10. **Effect of adsorbent dose on the adsorption of Cd^{2+}ions on the AS/Fe/AS nanocomposite.**

Effect of pH

It is known that Cd^{2+}ions are present in the form of Cd hydroxide in deionized water [20]. It was observed in FIG. 11, at pH 14, the efficiency of Cd^{2+} ions removal reaches up 90% at Cd^{2+} ions concentration of 11 mg/L. This phenomena can be explained by, when pH increases towered alkaline, the surface charge of (AS/Fe/AS) became negative charged and consequently, there is no electrostatic repulsion between the positively charged of Cd^{2+} ions and (AS/Fe/AS) surface, thereby, the adsorption of Cd^{2+} ions are increased [21], but at very alkaline pH solution, all Cd hydroxides are precipitate and inhibited the adsorption of Cd^{2+} ions on (AS/Fe/AS) surface, therefore, all the experiments were operated at pH 5.5. The increasing of pH solution after adsorption process may due to increase of the number of hydroxyl ions that released during interaction of nanocomposite magnetic adsorbents (AS/Fe/AS) with H_2O.

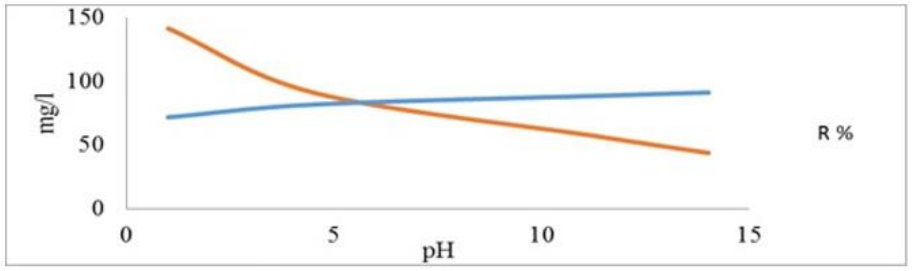

FIG. 11. **Effect of pH on the adsorption of Cd^{2+} ions on the AS/Fe/AS nanocomposite.**

Effect of contact time

In FIG. 12, the removal efficiency of Cd^{2+} ions was increased with increasing contact time, this can be attributed to the fact that discussed by Canela et al. [22], who reported that, once Cd^{2+} ions contacts with AS/ Fe/AS surface, they are removed immediately, but after the available active sites on AS/Fe/AS surface were completely filled, the ions become need longer time to reach other active sites on the surface of the adsorbent. We can say that, in order to get good results, Cd^{2+} ions should be contact on the surface of AS/Fe/AS nanocomposite for 36 min at least [23]. This result is important, because the equilibrium time, consider one of the most important parameters for an economical wastewater treatment system.

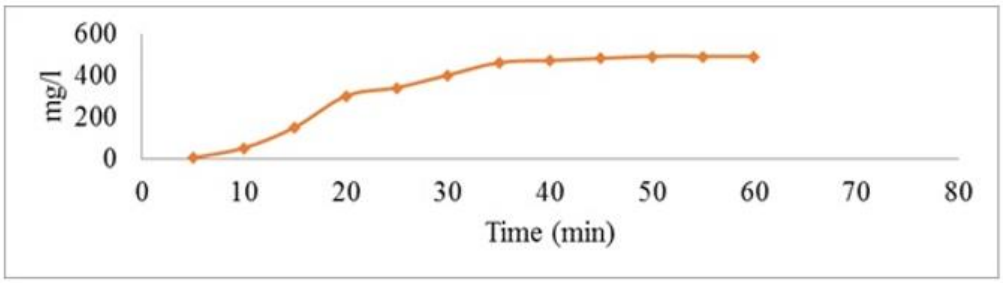

FIG. 12. **Effect of contact time on the adsorption of Cd^{2+} ions on the AS/Fe/AS nanocomposite.**

Effect of initial concentration: In FIG. 13, it's observed that, as the initial concentration was varied from 85 to 500 ppm, the corresponding efficiency were varied between 83 to 90.2%, respectively, where, all of pH, time, adsorbent dosage, and the temperature were kept constant. Also, we found that the removal efficiency and Cd^{2+} ions uptake increases with increasing initial concentration till 300 ppm, and above that concentration such change is not significant [24]. This shows that initial concentration has only a very little effect on adsorption [25].

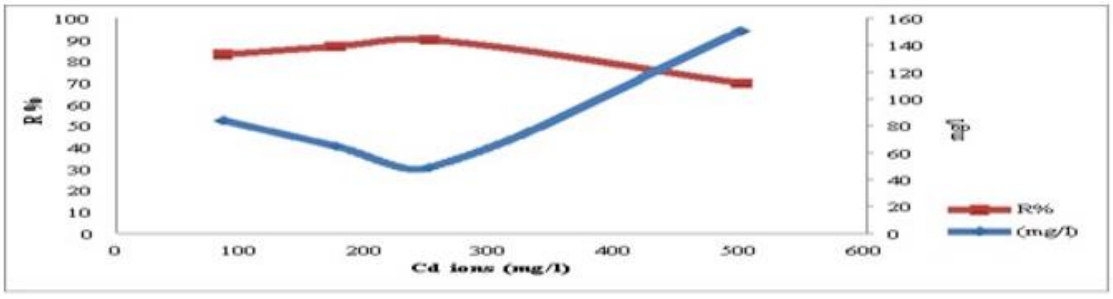

FIG. 13. **Effect of initial Cd^{2+} ions concentrations on the adsorption of cadmium ions on the AS/Fe/AS nanocomposite.**

Kinetics of adsorption

The adsorption kinetics behavior of uptakes Cd^{2+} ions by AS/Fe/AS nanocomposite, were understudied through the application of pseudo-first and pseudo-second-order kinetic models onto the batch adsorption results [26].

The linear form of the pseudo-first-order model can be expressed as:

$$\text{Log } (q_e - q_t) = \log qe - k_1 t/2.303 \quad (1)$$

where k_1 (min^{-1}) is the rate constant of the pseudo-first-order adsorption, and q_e and q_t (mg g^{-1}) are the adsorption capacities at equilibrium and at time t (min), respectively. The rate constants k_1, q_e and correlation coefficients r^2 were calculated using the slope and intercept of plots of lg ($q_e - q_t$) versus t, as shown in FIG. 14.

The pseudo-second-order rate expression is linearly expressed as:

$$t/qt = 1/k2q2e + t/qe \quad (2),$$

Anywhere, q_e and q_t equal the adsorption capacity at equilibrium and at time t (mg g^{-1}), and k_2 (g mg^{-1} min^{-1}), equal the rate constant of the pseudo-second-order adsorption. From the linear plots of t/q_t versus t, we can calculate the rate constants k_2, q_e and correlation coefficients r^2 (FIG. 15).

The parameters of two kinetic models that given in TABLE 1 indicating that, the correlation coefficient (r^2) of the pseudo-first-order kinetic model was 0.9211. Whereas, when we applying the pseudo-second-order kinetic model at 25°C, we found that, the correlation coefficient r^2 are ranged between 0.9989 to *1*, (or almost equal to 1) for all cases, i.e., this means that correlation coefficients (r^2) by applying the pseudo-second-order kinetic model, is much higher than the correlation coefficients derived from the pseudo-first-order. We can conclude that the both factors (r^2) and q_e, revealed that the adsorption of Cd^{2+} ions onto AS/Fe/AS nanocomposite followed the pseudo-second-order kinetic model, this indicating that the rate-limiting step between Cd^{2+} ions and the magnetic mesoporous silica nanocomposite is chemical adsorption process [27].

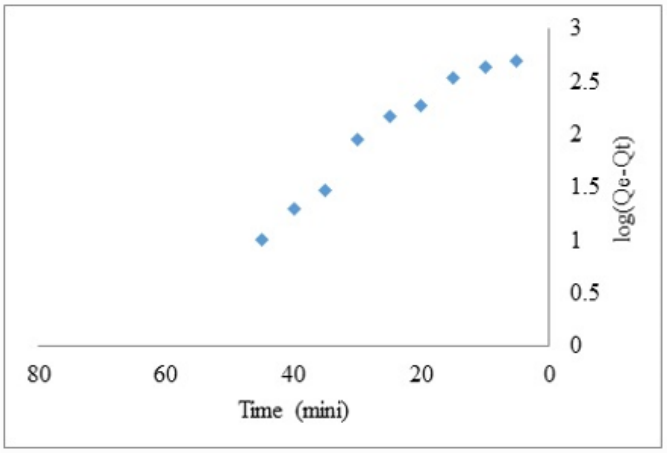

FIG. 14. **Pseudo-first-order adsorption of Cd^{2+} ions on AS/Fe/AS nanocomposites.**

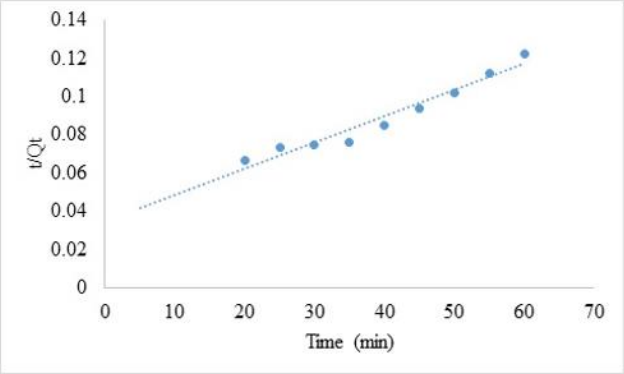

FIG. 15**. Pseudo-second-order adsorption of Cd^{2+} ions on AS/Fe/AS nanocomposites.**

TABLE 1. **Calculated kinetic parameters for the adsorption of Cd^{2+} ions onto AS/Fe/AS nanocomposites.**

Pseudo-first-order		**Pseudo-second-order**	
Models	**Cd^{2+} ions**	**Models**	**Cd^{2+} ions**
k_1 (min^{-1})	0.049	k_2 ($\times 10^{-3}$g mg^{-1} min^{-1})	3.98
q_{eq} (cal) (mg g^{-1})	20.5	q_{eq} (cal) (mg g^{-1})	350.9
r^2	0.9211	r^2	0.9989

Adsorption isotherm

Generally, adsorption isotherm is the relation between the quantities of adsorbate on the adsorbent as a function of its concentration under equilibrium conditions at constant temperature [28]. Moreover, the adsorption equilibrium is the most important information to understand and analysis the adsorption process [29]. The interaction between adsorbent and adsorbate are described by adsorption isotherms. Generally, adsorption isotherm is the relation between the quantities of adsorbate on the adsorbent as a function of its concentration under equilibrium conditions at constant temperature [28]. Thereby, the adsorption equilibrium is the most important information to understand and analysis the adsorption process. In this work, both models (Langmuir Isotherm and Freundlich Isotherm) were used to describe the relationship between the number of Cd^{2+}ions adsorbed and its equilibrium concentration in solution at room temperature.

Langmuir isotherm

The Langmuir equation may be written as the following;

$$Ce/Qe=1/(Qmb)+Ce/Qm, \quad (3)$$

noting that, we can defined this symbol as the following, Ce (mg/L) is the concentration of Cd^{2+}ions at equilibrium, and Qe (mg/g) means the amount of Cd^{2+} ions per unit mass of adsorbent (AS/Fe/AS nanocomposites) or means the adsorption capacity at equilibrium, Qm (mg/g) is the Langmuir constants related to the maximum adsorption capacity of Cd^{2+} ions on AS/Fe/AS nanocomposite surface, where, b (L/mg) is another Langmuir adsorption isotherm constant relates to the energy of adsorption (or rate of adsorption). If we linearity plotting of Ce/Qe versus Ce, we can calculated both Langmuir constants Qm

(mg/g) and b (L/mg) from the slope and intercept, respectively [30]. We can also express the fundamental properties of Langmuir isotherm in terms of a constant separation factor without dimensions (KL), which explains the shape and natural of Langmuir isotherm curves as written in the following equation

$$KL = (1/ (1+bCo), (4)$$

Somewhere, Co (mg/L) represented the maximum initial concentration of Cd^{2+} ions and b (L/mg) is Langmuir isotherm constant. From the equation 4, when the parameter KL>1 this means unfavorable adsorption, when 0<KL<1 means, favorable adsorption, when KL=0 this means irreversible adsorption, finally when, KL=1, it means a linear adsorption. The calculated Langmuir constants Qm and KL values are given in TABLE 2. From FIG. 16a and TABLE 2, we shown that the Langmuir constants Qm=0.82 mg/g, KL=0.007 and correlation coefficient (R^2)=0.636067. Accordingly, the KL values lay between, 0-1, this indicate a favorable adsorption for all initial Cd^{2+}ions concentrations (Co) and at studied temperatures.

Freundlich adsorption

On the other hand, the linear Freundlich adsorption isotherm can be represented by Equation (5)

$$\text{Log } Q_e = \log k_F + (1/n)\ log\ C_{eq}, (5),$$

Where both of k_F and n are the Freundlich constants and C_{eq} is the concentration of Cd^{2+} ions at equilibrium (mg L^{-1}). From Equation 5, both of K_F and n values, can be calculated experimentally from plotting of log Q_{eq} versus log C_{eq}, thereby, the equilibrium isotherm data that fitted with Freundlich equation are illustrated in FIG. 16b, we found that the K_f and n values, are 2.037 and 3.0029, respectively [31]. We, found also, that the correlation coefficient value (R^2) are equal one in case of Freundlich, compared to 0.636067 in case of Langmuir.

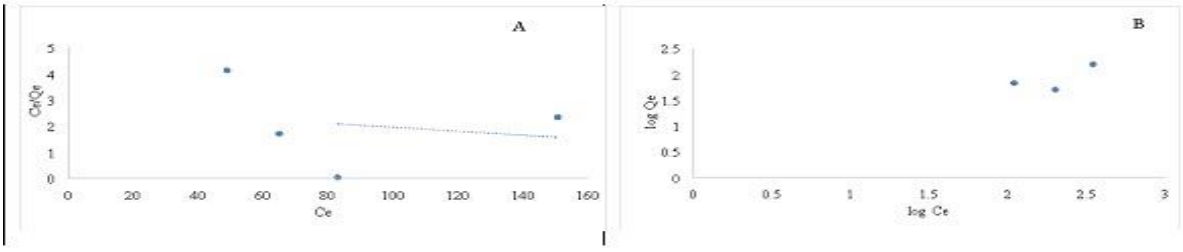

FIG. 16. **Langmuir (a) and Freundlich (b) adsorption isotherm of Cd^{2+} ions onto AS/Fe/AS nanocomposites.**

In this work, both Langmuir Isotherm and Freundlich Isotherm were applied to describe the relationship between the number of Cd^{2+} ions adsorbed and its equilibrium concentration in solution at room temperature and the results are presented in TABLE 2.

TABLE 2. **The calculated Langmuir and Freundlich Isotherm.**

Isotherm equation	Langmuir	Isotherm equation	Freundlich
Qm (mg g^{-1})	0.826557	k f	2.037434
KL (L mg^{-1})	0.007297	n	3.002945
R^2	0.636067	R^2	1

Mechanism of adsorption process

As shown in FIG. 17, the AS/Fe/AS nanocomposite is composed of three layers, the first one, is the micro silicon oxide layer which located in the core of composite, and covered by second magnetic iron oxide layer, which consisted of zero valent iron and spinning magnetic iron oxide (Fe_3O_4). The second iron layer possess a variable functional hydroxyl groups, which having an ability as ion exchange and coordination bond, both working together and enhancing the strength of the magnetic layer towered adsorption of heavy metals. The third layer is composed of silicon oxide sheet as semi permeable membrane to adsorb ions under study; such layered give a selectivity to the nanocomposite toward adsorption of heavy metals. The adsorption capacity of Cd^{2+} ions using silica nanocomposite ranged between 50-73.16 mmol/100 g) as reported in [31], meanwhile, our nanocomposite (AS/Fe/AS) have an adsorption Cd^{2+} ions affinity of 100 mmol/100 g. This indicating to how the compatibility of our prepared nanocomposite with each other, which increases and enhance their ability to exchange ions, especially in the field of water treatment from heavy elements.

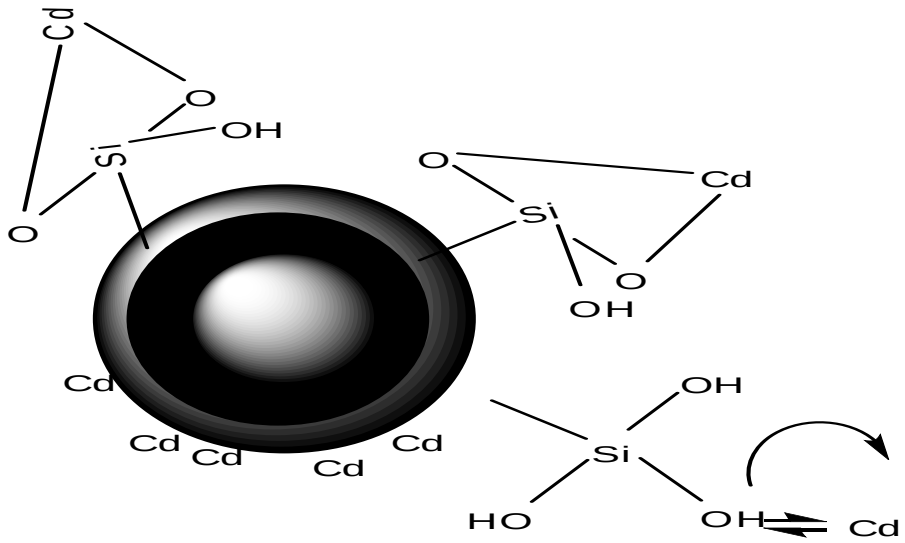

FIG. 17. **Mechanism of Cd^{2+} ions adsorption on the AS/Fe/AS nanocomposite.**

Novelty of our nanocomposite (AS/Fe/AS)

Mesoporous silica nanoparticles (MSNs), specifically Mobil Crystalline Materials (MCM-41), SiO_2, hollow silica and Santa Barbara Amorphous type material (SBA-15), have gained wide popularity over the recent years due to their uniform and tunable pore size, easy independent functionalization of the surface, internal and external pores, high specific surface area and chemical stability, making it a distinctive and promising carrier materials [32]. In the past few years, a lot of works of combination of Fe_3O_4 and silica frameworks to form a catalytic material were reported. For example, Kevan and coworkers incorporated Fe_3O_4 into SBA-15 via incipient-wetness impregnation with $FeCl_3$ in ethanol followed by calcinations. The adsorption and degradation of methylene blue and other metal ions like Ni, Zn, Cr ions by a novel catalytic Fe_3O_4/SiO_2 nanocomposite, was reported by Hassan et al. In fact, numbers of similar studies have demonstrated that the silica supported Fe_3O_4 could present better adsorption performance than traditional materials.

Our product AS/Fe/AS nanocomposite were compared with the other nano-composite in the literature [33-35], and we found that our product AS/Fe/AS nanocomposite are very promising and give removal efficiency of 85-90% at very high Cd^{2+} ions concentrations reach to 500 ppm, where the other nanocomposite in the literature remove only low pollutant concentrations reach to 50 ppm [33-35].

Conclusion

Magnetic core shell AS/Fe/AS nano-composites was synthesized to remove divalent cadmium ions from contaminated water. The effect of initial concentration, adsorbent dosage, pH and time were studied at a constant temperature of 30°C. Comparing the regression coefficients reveal that the sorption of Cd^{2+} ions onto AS/Fe/AS nanocomposites can be successfully described by the pseudo-second order kinetic model and Freundlich adsorption isotherm. We found that the Cd^{2+} ions were successfully removed by adsorption onto AS/Fe/AS nanocomposites. Accordingly, in future we can impregnate our nanocomposites in a suitable matrix to form a polymer nanocomposite.

REFERENCES

1. Tayel AA. Nanometals appraisal in food preservation and food-related activities A2 - Grumezescu, Alexandru Mihai, in Food Preservation. Academic Press. 2017;pp:487-526.
2. Barnett MO, Kent DB. Adsorption of metals by geomedia II: variables, mechanisms, and model applications. 1st ed. Developments in earth and environmental sciences. Amsterdam, Boston: Elsevier. 2008;p:478.
3. Zub YI. Metal phthalocyanines fixed onto polyorganosiloxane matrices as oxidation catalysts for HS groups. Catalysis Today. 1993;17 (1-2):31-9.
4. Jiang L, Liu P, Zhao S. Magnetic ATP/FA/Poly (AA-co-AM) ternary nanocomposite microgel as selective adsorbent for removal of heavy metals from wastewater. Colloids and Surfaces A: Physicochemical and Engineering Aspects. 2015;470:31-8.
5. Amirnia S, Ray MB, Margaritis A. Heavy metals removal from aqueous solutions using Saccharomyces cerevisiae in a novel continuous bioreactor–biosorption system. Chem Eng J. 2015;264:863-72.
6. Duman O. Removal of triphenylmethane and reactive azo dyes from aqueous solution by magnetic carbon nanotube-κ-carrageenan-Fe_3O_4 nanocomposite. Journal of Alloys and Compounds. 2016;687:370-83.
7. Wu X. Effect of the rare-earth substitution on the structural, magnetic and adsorption properties in cobalt ferrite nanoparticles. Ceramics Int. 2016;42 (3):4246-55.
8. Chen X. Exploring beyond palladium: Catalytic reduction of aqueous oxyanion pollutants with alternative platinum group metals and new mechanistic implications. Chem Eng J. 2017;313:745-52.
9. Zewail TM, Yousef NS. Kinetic study of heavy metal ions removal by ion exchange in batch conical air spouted bed. Alexandria Eng J. 2015;54 (1):83-90.
10. Wang Z. Silica oxide encapsulated natural zeolite for high efficiency removal of low concentration heavy metals in water. Colloids and Surfaces A: Physicochemical and Engineering Aspects. 2019;561:388-94.
11. He Y. Electromagnetic wave absorbing cement-based composite using Nano-Fe_3O_4 magnetic fluid as absorber. Cement and Concrete Composites. 2018;92:1-6.
12. Gifford M. Phosphorus recovery from microbial biofuel residual using microwave peroxide digestion and anion exchange. Water Res. 2015;70:130-7.

13. Fathy M, Mousa TAM, Abdel-Hameed AA. Sulfonated ion exchange polystyrene composite resin for calcium hardness removal. Int J Emerging Technol Adv Eng. 2015;5 (10):20-9.
14. Fathy M, Abdel-Hameed AA. Synthesis and characterization of cellulose nanoparticles obtained from rice straw waste. Int J Mod Org Chem. 2015;4 (1):56-61.
15. Fathy M, Elsayed A. Preparation of cation-exchange resin from styrene-divinylbenzene copolymer obtained by suspension polymerization method. Elixir Int J. 2014.
16. Min KA, Hong S. Doping effect in graphene on oxide substrates: MgO (111) and SiO2 (0001). Current Applied Physics, 2015;15:S103-S7.
17. Han S, Li X, Wang Y, et al. Multifunctional imprinted polymers based on CdTe/CdS and magnetic graphene oxide for selective recognition and separation of p-t-octylphenol. Chem Eng J. 2015;271:87-95.
18. Pathipati SR, Pavlica E, Parvez K, et al. Graphene flakes at the SiO_2/organic-semiconductor interface for high-mobility field-effect transistors. Organic Electronics. 2015;27:221-6.
19. Naim MM, Monir AA. Desalination using supported liquid membranes. Desalination. 2003;153 (1-3):361-9.
20. Meng J, Cao Y, Suo Y, et al. Facile Fabrication of 3D SiO_2@Graphene Aerogel Composites as Anode Material for Lithium Ion Batteries. Electrochimica Acta. 2015;176:1001-9.
21. Zuo X, Shi W, Tian Z, et al. Desalination of water with a high degree of mineralization using SiO_2/PVDF membranes. Desalination. 2013;311:150-5.
22. Canela N, Herrero P, Marine S, et al. Analytical methods in sphingolipidomics: Quantitative and profiling approaches in food analysis. J Chromatography A. 2006.
23. Bao S, Tang L, Li K. Highly selective removal of Zn (II) ion from hot-dip galvanizing pickling waste with amino-functionalized Fe_3O_4@SiO_2 magnetic nano-adsorbent. J Colloid and Interface Sci. 2016;462:235-42.
24. Banazadeh A, Mozaffari S, Osoli B. Facile synthesis of cysteine functionalized magnetic graphene oxide nanosheets: application in solid phase extraction of cadmium from environmental sample. J Environ Chem Eng. 2015;3 (4):2801-8.
25. Zhang Z, Zhang H, Zhu L, et al. Hierarchical porous Ca $(BO_2)_2$ microspheres: Hydrothermal-thermal conversion synthesis and their applications in heavy metal ions adsorption and solvent-free oxidation of benzyl alcohol. Chem Eng J. 2016;283:1273-84.
26. Huang YD, Gao XD, Gu ZY, et al. Amino-terminated SiO_2 aerogel towards highly-effective lead (II) adsorbent via the ambient drying process. J Non-Crystalline Solids. 2016;443:39-46.
27. Zhu Z, Xie J, Zhang M, et al. Insight into the adsorption of PPCPs by porous adsorbents: Effect of the properties of adsorbents and adsorbates. Environmental Pollution. 2016;214:524-31.
28. Ramzi M, El-Sayed RHM, Fathy M, et al. Evaluation of scale inhibitors performance under simulated flowing field conditions using dynamic tube blocking test. Int J Chem Sci. 2016;14 (1):16-28.
29. Ali ES, Alsaman AS, Harby K, et al. Recycling brine water of reverse osmosis desalination employing adsorption desalination: A theoretical simulation. Desalination. 2017;408:13-24.
30. Ravishankar H, Wang J, Shu L, et al., Removal of Pb (II) ions using polymer based graphene oxide magnetic nano-sorbent. Process Safety and Environmental Protection. 2016;104:472-80.
31. Sun W, Li L, Luo C, et al. Synthesis of magnetic graphene nanocomposites decorated with ionic liquids for fast lead ion removal. International Journal of Biological Macromolecules. 2016;85:246-51.

32. El-Maghrabi H, Hosny R, Ramzi M, et al. Novel mesoporous silica (MCM-41) and its characterization for oil adsorption from produced water injected in water injection projects using fixed bed column processes. Desalination and Water Treatment. 2017;60:70-7.
33. Ebisike K, Okoronkwo AE, Alaneme KK. Adsorption of Cd (II) on chitosan-silica hybrid aerogel from aqueous solution. Environ Technol and Innovation. 2019;14:p.100337.
34. Wu D, Wang Y, Li Y, et al. Phosphorylated chitosan/$CoFe_2O_4$ composite for the efficient removal of Pb (II) and Cd (II) from aqueous solution: Adsorption performance and mechanism studies. J Mol Liq. 2019;277:181-8.
35. Karnib M, Kabbani A, Holail H, et al. Heavy Metals removal using activated carbon, silica and silica activated carbon composite. Energy Procedia. 2014;50:113-20.